3D modelling of in-stent restenosis

Zun, P.

Publication date
2019
Document Version
Other version
License
Other

[Link to publication](#)

Citation for published version (APA):
Zun, P. (2019). *3D modelling of in-stent restenosis*. [Thesis, fully internal, Universiteit van Amsterdam].

Summary:

Coronary artery disease is one of the most widespread causes of mortality in industrialized countries. Coronary artery stenosis, or abnormal narrowing, can lead to ischemia and potentially fatal heart attacks. This narrowing is often corrected by deploying a metal mesh called a stent in the affected artery to keep it open and maintain blood flow. After stenting, cells in the wounded vessel wall start growing and proliferating. Excessive proliferation can lead to a repeat narrowing, or restenosis, which adversely affects coronary blood supply. Computational models can be used to better understand this process.

In this thesis a fully-coupled 3D multiscale computational model of in-stent restenosis is developed, which describes the process of post-stenting tissue growth, and is validated against *in vivo* and *in vitro* data. Also, the model's uncertainties and the assumed boundary conditions are studied.

This multiscale model includes single-scale models for stent deployment, blood flow, and tissue growth in the stented vessel, including smooth muscle cell (SMC) proliferation and extracellular matrix (ECM) production. The blood flow model is fully coupled to the tissue growth model. The model is validated using data from porcine *in vivo* experiments, first by comparing growth in a simulated vessel to growth in a similarly injured porcine vessel, and then by simulating stent deployment using data obtained from micro computed tomography (micro-CT) and directly comparing the simulation results of neointimal growth to histological sections taken at the same locations. To the best of our knowledge, this is the first time that such a detailed validation of a fully coupled three-dimensional model of ISR against detailed histological data has been performed.

Uncertainty quantification and sensitivity analysis is performed on a simplified 2D model of in-stent restenosis to determine the effect of the model's parameters and variances in physiology on neointimal growth. The sensitivity analysis suggests that two major factors that affect restenosis are the wall shear stress in the stented segment and post-operational endothelium recovery. Because of this, two other separate *in silico* models are developed to study the effects of flow boundary conditions and variances in coronary anatomy on cell proliferation in a simplified 2D stented vessel, and also endothelial cell (EC) migration *in vitro* under flow conditions, which can clarify the details of endothelial recovery *in vivo*.

The model of EC migration is particle-based. Cell movement in the model is a combination of random walks and directed movement along the local flow velocity vector. For model calibration and validation, a set of experimental data for cell migration in a rectangular ridged channel has been used. We have first calibrated the model for a baseline case of a channel with no obstacles, and then applied it to the case of a channel with ridges on the bottom surface, representative of stent strut geometry. The modelling results support the hypothesis that EC movement is strongly affected by local wall shear stress direction and magnitude, and also explain the behaviour reported in an earlier work, where the authors attributed cell migration to minimization of shear stress gradient. Our results show that this hypothesis is not required to reproduce *in vitro* observations of cell migration.

The study of flow boundary conditions was done by coupling a 2D model of ISR to a 1D model of an entire human coronary tree. The restenosis dynamics for the assumptions of a constant flow and a constant pressure drop across the coronary tree were considered. The simulations showed no significant difference in neointimal growth between the two assumptions for most locations in the coronary tree, and the differences can only be observed at the locations where a strong alternative flow pathway is present.

On the other hand, the difference between locations is significant, which is consistent with small vessel size being a clinical risk factor for restenosis. These results also suggest that assumption of constant flow is a good approximation for ISR models dealing with the typical progression of ISR in the most often stented locations such as the proximal parts of LAD and LCX.

For the detailed validation study, metrics for comparison are per-strut neointimal thickness and per-section neointimal area. The neointimal area predicted by the model demonstrates a good agreement with the detailed experimental data. For 14 days post-stenting the relative neointimal area, averaged over all vessel sections considered, was 20±3% *in vivo* and 22±4% *in silico*. For 28 days, the area was 42±3% *in vivo* and 41±3% *in silico*.

The model was able to closely match both validation datasets with a single set of parameters. It should be noted that including vessel curvature and ECM production in the model was paramount to obtain a good agreement with the experimental data. Based on these results, we now consider the model validated for the case of BMS implantation in a healthy porcine coronary artery.

Samenvatting:

Coronaire hartziekte is een van de meest voorkomende doodsoorzaken in geïndustrialiseerde landen. Vernauwing van de kransslagader kan leiden tot ischemie en mogelijk fatale hartaanvallen. Deze vernauwing wordt vaak gecorrigeerd door het gebruik van een metalenbusje, een stent genaamd, om deze open te houden en de bloedstroom in stand te houden. Na het plaatsen van een stent beginnen de cellen van de beschadigde vaatwand te groeien en zich te vermenigvuldigen. Overmatige proliferatie kan leiden tot een herhaalde vernauwing, of restenose, die een negatieve invloed heeft op de coronaire bloedtoevoer. Computermodellen kunnen worden gebruikt om dit proces beter te begrijpen.

In dit proefschrift wordt een volledig-gekoppeld 3D multi-schaal rekenmodel van in-stent restenose (ISR) ontwikkeld, dat het proces van weefselgroei na het plaatsen van een stent beschrijft, en gevalideerd wordt aan de hand van in vivo en in vitro data. Ook worden de onzekerheden van het model en de veronderstelde randvoorwaarden bestudeerd.

Dit multi-schaal model omvat enkel-schaalmodellen voor de plaatsing van de stent, de bloedstroom en de weefselgroei in het bloedvat, met inbegrip van de proliferatie van gladde spiercellen (SMC) en de productie van extracellulaire matrix (ECM). Het bloedstrommodel is volledig gekoppeld aan het weefselgroeimodel. Het model wordt gevalideerd aan de hand van gegevens uit in vivo experimenten, eerst door de groei in een gesimuleerd vat te vergelijken met de groei in een gelijkaardig beschadigd varkensvat, en vervolgens door het simuleren van de plaatsing van de stent met behulp van gegevens verkregen uit microcomputertomografie (microCT) en het direct vergelijken van de simulatieresultaten van de neo-intimale groei met histologische secties genomen op dezelfde locaties. Voor zover bij ons bekend, is dit de eerste keer dat een dergelijke gedetailleerde validatie van een volledig gekoppeld driedimensionaal model van ISR aan de hand van gedetailleerde histologische gegevens is uitgevoerd.

Onzekerheidskwantificering en sensitiviteitsanalyse wordt uitgevoerd op een vereenvoudigd 2D model van in-stent restenose om het effect van de parameters van het model en variaties in de fysiologie op de neo-intimale groei te bepalen. De sensitiviteitsanalyse suggereert dat twee belangrijke factoren zijn die restenose beïnvloeden: de afschuifspanning in het segment met de stent en het postoperatieve

endotheelherstel. Om deze reden worden twee afzonderlijke in silico modellen ontwikkeld om de effecten van grensvoorwaarde en varianties in de coronaire anatomie op de celproliferatie in een vereenvoudigd 2D bloedvat te bestuderen, en ook endotheelcel (EC) migratie in vitro onder flow condities, wat de details van endotheelherstel in vivo kan verduidelijken.

Het model van EC migratie is gebaseerd op deeltjes. De celbeweging in het model is een combinatie van willekeurige wandelingen en gerichte beweging langs de lokale snelheidsvector. Voor de kalibratie en validatie van het model is gebruik gemaakt van een set van experimentele gegevens voor celmigratie in een rechthoekig geribbeld kanaal. We hebben het model eerst gekalibreerd voor een kanaal zonder obstakels, en vervolgens toegepast op een kanaal met ribbels op de bodem, representatief voor de geometrie van de stentstang. De modelleringsresultaten ondersteunen de hypothese dat de EC beweging sterk beïnvloed wordt door de richting en grootte van de lokale afschuifspanning en verklaren ook het gedrag dat gerapporteerd werd in een eerder werk, waar de auteurs de celmigratie toeschreven aan het minimaliseren van de afschuifspanningsgradiënt. Onze resultaten tonen aan dat deze hypothese niet nodig is om in vitro observaties van celmigratie te reproduceren.

De studie naar de randvoorwaarden werd door uitgevoerd her koppelen van een 2D model van ISR aan een 1D model van een volledig menselijk coronair vaatstelsel. De restenose dynamiek voor de aannames van een constante flow en een constante drukval over het coronair vaatstelsel werden overwogen. De simulaties toonden geen significant verschil in neo-intimale groei tussen de twee aannames voor de meeste plaatsen in het coronair vaatstelsel, en de verschillen kunnen alleen worden waargenomen op de plaatsen waar een sterke alternatieve stroomroute aanwezig is.

Aan de andere kant is het verschil tussen de locaties significant, dit is consistent met het feit dat de kleine vaatgrootte een klinische risicofactor voor restenose is. Deze resultaten suggereren ook dat de aanname van een constante stroming een goede benadering is voor ISR modellen die de typische progressie van ISR in de meest voorkomende locaties van een stent zoals de proximale delen van LAD en LCX beschrijven.

Voor de gedetailleerde validatiestudie zijn de vergelijkingsmaatstaven per-steun neo-intimale dikte en per sectie neo-intimal gebied. Het door het model voorspelde neo-intimal gebied toont een goede overeenkomst aan met de gedetailleerde experimentele gegevens. Gedurende 14 dagen na het plaatsen van de stent bedroeg het relatieve neo-intimal gebied, gemiddeld over alle betrokken vaatdelen, 20±3% in vivo en 22±4% in silico. Gedurende 28 dagen was het gebied 42±3% in vivo en 41±3% in silico.

Het model was in staat om beide validatiedatasets met één enkele set parameters nauw op elkaar af te stemmen. Opgemerkt moet worden dat het opnemen van de kromming van de vaten en de ECM-productie in het model van het grootste belang was om een goede overeenstemming met de experimentele gegevens te verkrijgen. Op basis van deze resultaten beschouwen we het model nu als gevalideerd voor het geval van BVK-implantatie in een gezonde kransslagader van varkens.

Краткое содержание:

Заболевания коронарных артерий являются одной из самых распространенных причин смерти в индустриализованных странах. Стеноз — это аномальное сужение коронарных артерий, которое может привести к ишемии и к потенциально смертельным сердечным приступам. Такое сужение артерий часто корректируется установкой металлической сетки – стента – в пораженную артерию для увеличения просвета артерии и восстановления кровотока. После стентирования клетки в поврежденной стенке артерии начинают процесс роста и пролиферации. Чрезмерная пролиферация клеток может привести к повторному сужению, или рестенозу, который отрицательно влияет на кровоснабжение сердечной мышцы. Для лучшего понимания этого процесса могут быть использованы компьютерные модели.

В данной диссертации разработана полностью сопряженная трехмерная компьютерная модель внутристентового рестеноза (ВСР), которая описывает процесс роста ткани после стентирования, и которая валидируется с помощью данных экспериментов in vivo и in vitro. Кроме того, изучаются имеющиеся в модели неопределенности и используемые граничные условия.

Данная многомасштабная модель включает в себя модели раскрытия стента, кровотока и роста ткани в стентированном сосуде, при этом модель роста ткани включает пролиферацию гладкомышечных клеток (ГМК) и секрецию внеклеточного матрикса (ВКМ). Модель кровотока полностью сопряжена с моделью роста ткани. Многомасштабная модель валидируется с помощью данных экспериментов на свиньях in vivo, вначале путем сравнения роста в модельном сосуде с ростом в так же поврежденном сосуде in vivo, а затем путем моделирования раскрытия стента с помощью данных, полученных путем микро-компьютерной томографии (микро-КТ) стента и прямого сравнения результатов моделирования роста неоинтимы с гистологическими срезами тех же участков сосуда. Насколько нам известно, это первое настолько детальное валидационное исследование трехмерной компьютерной полностью сопряженной модели ВСР на основе подробны гистологических данных.

Оценка неопределенности и анализ чувствительности проводятся на упрощенной двумерной модели ВСР, для того чтобы определить эффект модельных параметров и

вариаций физиологии на рост неоинтимы. Анализ чувствительности указывает на два основных фактора, которые влияют на рестеноз: сдвиговое напряжение на стенке сосуда и послеоперационное восстановление эндотелия. По этой причине, две отдельные компьютерные модели были разработаны для изучения эффектов граничных условий кровотока и вариаций коронарной анатомии на пролиферацию в упрощенной двумерной версии стентированного сосуда, а также миграции клеток эндотелия (ЭК) in vitro в условиях течения в сосуде, что поможет прояснить детали восстановления эндотелия in vivo.

Модель миграции ЭК представляет отдельные клетки в виде частиц. Движение клеток в этой модели – это комбинация случайных блужданий и направленного движения под действием локального течения. Для калибровки и валидации модели используется набор экспериментальных данных о миграции клеток в прямоугольном канале с препятствиями. Вначале модель была откалибрована для базового случая канала с плоским дном, а затем применена к случаю канала с ребрами на нижней поверхности, соответствующими геометрии волокон стента. Результаты моделирования поддерживают гипотезу того, что движение ЭК в значительной степени определяется направлением и величиной локального сдвигового напряжения, и также объясняет поведение клеток, описанное в более ранней работе, где авторы объясняли миграцию клеток минимизацией градиента сдвигового напряжения. Наши результаты показывают, что данная гипотеза не обязательна для воспроизведения в компьютерной модели движения клеток in vitro.

Исследование граничных условий проводилось путем сопряжения двумерной модели ВСР с одномерной моделью тока крови в коронарных сосудах. Была рассмотрена динамика рестеноза для предположений постоянного потока и постоянного давления в аорте. Моделирование показало отсутствие значимых различий в росте неоинтимы для большей части рассмотренных сосудов, и различия наблюдаются только в тех местах, где присутствует крупный обходной канал течения.

С другой стороны, различия между разными точками коронарных артерий весьма значительны, что согласуется с тем, что малый размер сосуда является клиническим фактором риска рестеноза. Эти результаты также указывают на до, что приближение постоянного потока является хорошей аппроксимацией для моделей ВСР, рассматривающих типичное развитие рестеноза в наиболее часто стентируемых местах, таких как проксимальные части передней межжелудочковой артерии (ПМЖА) и огибающей артерии (ОА).

Для детального валидационного исследования в качестве метрик для сравнения были выбраны толщина неоинтимы поверх отдельных волокон стента и площадь неоинтимы на срезах. Предсказанная моделью площадь неоинтимы хорошо соотносится с экспериментальными результатами. Для 14 дней после стентирования относительная площадь неоинтимы, усредненная по всем рассмотренным срезам, составила 20±3% *in vivo* и 22±4% *in silico*. Для 28 дней площадь составила 42±3% *in vivo* и 41±3% *in silico*.

Модель смогла достаточно точно воспроизвести оба набора валидационных данных с использованием одного набора параметров. Надо отметить, что включение в модель секреции ВКМ и изогнутой геометрии сосуда оказалось необходимым для хорошего воспроизведения экспериментальных данных. На основе этих результатов модель мы считаем модель валидированной для случая здоровой коронарной артерии свиньи, стентированной металлическим стентом.

Acknowledgements

The work in this thesis has been made possible by help and support from many different people around me, who have aided me, in very diverse ways, over the course of these past four years.

First of all, I would like to thank my supervisors: Alfons Hoekstra at UvA, Alexander Boukhanovsky and Andrew Svitenkov at ITMO, for making this joint program possible and for guiding my research these past four years. I think the joint PhD program between ITMO and UvA is an extremely cool thing, and I hope that more people will be able to take part in it.

The work described here builds upon earlier studies by a number of people. I thank Hannan Tahir, David Evans, Joris Borgdorff, Carles Bona-Casas and Bernd Stahl for their contributions to the initial 2D ISR model and to the 3D prototype.

I thank my colleagues at ITMO and UvA for helpful discussions and for being generally great people to be around. In particular, I thank Alva for being in the joint PhD program together with me and going through the same changing and mildly confusing steps (it is a new program after all). It has been reassuring to not be the only person dealing with these non-standard arrangements. Also, thank you for helping with the paperwork in Petersburg when I wasn't there to do it myself.

Lourens, thank you for your tremendous help with the technical side of things and getting the 2D models running again.

Britt, thank you for proofreading and correcting the Dutch summary of this manuscript. Victor, thanks for showing me around the university and the Universum.

Amir, thanks for the talks about curious applications of neural networks and for inviting me to help organize that programming contest. That was a fun experience.

Gabor and Vishnu, thanks for the game nights. Ben, David, Raymond, Anna, Dongwei, thank you for being generally cool people to be around.

Valeria, Grace, thank you for your help with the more formal side of preparing my thesis.

I would like to end this thesis with a quote from Michael Faraday: "Nothing is too wonderful to be true, if it be consistent with the laws of nature; and in such things as these, experiment is the best test of such consistency".

List of publications

Journal papers:

1.   Zun PS, Anikina T, Svitenkov A, Hoekstra AG. A Comparison of Fully-Coupled 3D In-Stent Restenosis Simulations to In-vivo Data // Front Physiol 2017. №8. P. 284.

DOI: http://dx.doi.org/10.3389/fphys.2017.00284

Contributions: PSZ implemented the current version of the model, designed and performed the simulations for variable injury score and variable reendothelization speed, analysed the results and wrote the manuscript.

2.   Zun PS, Hoekstra AG. On the Possible Interaction Mechanism between Collateral Vessels and Restenosis // Procedia Comput Sci 2015. №66. P. 412–8.

DOI: http://dx.doi.org/10.1016/j.procs.2015.11.047

Contributions: PSZ designed and implemented the model, performed the analytical estimation and wrote the manuscript.

3.   Hoekstra AG, Alowayyed S, Lorenz E, Melnikova N, Mountrakis L, Rooij B van, Svitenkov A, Zavodszky G, Zun P. Towards the Virtual Artery: a Multiscale Model for Vascular Physiology at the PCB Interface // Phil Trans R Soc A 2016. №374. P. 20160146.

DOI: http://dx.doi.org/10.1098/rsta.2016.0146

Contributions: PZ contributed to the research on the ISR, drafted and revised that part of the manuscript and created figure 2. He also contributed to the conception of the concept of the virtual artery and revised those sections of the manuscript.

4.   Nikishova A, Veen L, Zun P, Hoekstra AG. Uncertainty Quantification of a Multiscale Model for In-Stent Restenosis // Cardiovasc Eng Technol 2018. №9. P. 761–74.

DOI: http://dx.doi.org/10.1007/s13239-018-00372-4

Contributions: PZ adapted the ISR2D model for uncertainty quantification, designed the study, implemented a new flow model, and helped draft the manuscript.

5.   Nikishova A, Veen L, Zun P, Hoekstra AG. Semi-intrusive multiscale metamodelling uncertainty quantification with application to a model of in-stent restenosis // Philos. Trans. R. Soc. A Math. Phys. Eng. Sci. 2019. Vol. 377, № 2142. P. 20180154.

DOI: http://dx.doi.org/10.1098/rsta.2018.0154

Contributions: PZ helped to design the study, adapted the ISR2D model, and helped to draft the manuscript.

6.   Svitenkov A, Zun P, Rekin O, Hoekstra AG. Partitioning of Arterial Tree for Parallel Decomposition of Hemodynamic Calculations // Procedia Comput Sci 2016. №80. P. 977–87.

DOI: http://dx.doi.org/10.1016/j.procs.2016.05.393

Contributions: PZ implemented the spectral graph partitioning algorithms, set up the computational experiments and helped draft the manuscript.

Planned:

1.   Zun P, Narracott AJ, Chiastra C, Gunn J, Hoekstra AG. Location-specific comparison between a 3D in-stent restenosis model and micro-CT and histology data from porcine *in vivo* experiments // Accepted for publication in Cardiovasc Eng Technol, 2019.

DOI: http://dx.doi.org/10.1007/s13239-019-00431-4

Contributions: PZ implemented the current version of the model, designed and performed the simulations, analysed the results and drafted the manuscript.

2.   Zun P, Narracott AJ, Evans P, Hoekstra AG. A model for endothelial cell migration under flow conditions // Under review at Biomech. and Mod. Mechanobiol., 2019.

Contributions: PZ designed and implemented the model, designed and performed the simulations, analysed the results and drafted the manuscript.

3.   P.S. Zun, L.E. Veen, A.I. Svitenkov, A.G. Hoekstra. Effects of Local Coronary Blood Flow Dynamics on the Predictions of a Model of In-stent Restenosis // Paper under preparation.

Contributions: PZ adapted the 2D ISR model for the study, designed and implemented the 1D-2D coupling, designed and performed the simulations, analysed the results and drafted the manuscript.

Appendix A.
Parameters used in the model

#	Name	Value porcine	Value human	Comments
1	Inner diameter	2.8 mm [131]	3.6±0.4 mm [136,137]	Porcine data is what is currently used in the simulation (Yorkshire minipig RCA); human value based on the middle of LAD segment before the first bifurcation for balanced hearts
2	Outer diameter	3.3 mm [131]	4.5±0.3 mm [66]	Human value includes adventitia; porcine does not
3	Wall thickness	0.25 mm [138]	0.85 mm A+M+I; 0.3 mm M only; 0.5 mm M+I; (calc. from [66])	Holzapfel et al.: "The ratio of outer diameter to total wall thickness was 0.189 ± 0.014; ratios of adventitia, media, and intima thickness to total wall thickness were 0.4 ± 0.03, 0.36 ± 0.03, and 0.27 ± 0.02" A – adventitia, M – media, I – intima. NB: Most arteries were diseased.

#	Name	Value porcine	Value human	Comments
4	Blood velocity	0.15 m/s [139]	0.40±0.19 m/s [93]	Average velocity at the center of the vessel Ofili et al.: 6 LMA, 7 LAD, 4 LCX Huo et al.: 5-14 cm/s in porcine RCA during cardiac cycle
5	Endothelium regeneration time	14 days [72,73] Healthy vessels See comment section for details	Early BMS, implanted in 1995-97 [116] Diseased vessels Up to 16 days: complete destruction 6 weeks: continuous SMC-rich neointima 61 days: no recovery yet; 12 weeks (84, 96 days): recovery	Porcine: 53±36% after 2 days, 95±2% after 5 days, 99±2% after 14 days – EC coverage 59±25% after 3 days, 96±7% after 14 days (data over struts, used in porcine model) – PECAM-1 (platelet endothelial cell adhesion molecule) aka CD31 Between struts: 81±14%, 100±0% respectively [72]. Data for Genous stent was used instead of BMS. The reasoning was that the Genous stent accelerates reendothelization, but does not reduce the hyperplasia, hence it is assumed extra ECs are dysfunctional, and PECAM-1 expression is the same as BMS

#	Name	Value porcine	Value human	Comments
6	Curvature radius	28-36 mm [131] Degree of the curve ~39-51° for a 25 mm segment	Calculated, see comment. For average values, radius is $\frac{180\cdot10.2}{\pi\cdot52} = 11\ cm$ (whole RCA) For proximal RCA, R is up to $57.3 \cdot \frac{4.7}{55} = 5\ cm$ (or less)	Degree of curve: 30-66°, avg. 52°±9 Length: 10.2±1.7 cm (5.7-14.5 cm) [130]
7	SMC cell cycle	32 hours [138]	Similar	The doubling time in human arterial SMCs in vitro ranges between 24-48 hours for different setups [140–142]. Some SMCs in the cultures are likely inhibited; low doubling time requires a load of PDGF
8	SMC agent radius	0.015 mm [29,138]		Radius is an estimation (SMCs are not round in reality) Probably the same radius is a good approximation
9	NO production rate	See [138,143] for NO in relation to WSS		For more detailed data see source; porcine data for pig hind limbs of varying size

#	Name	Value porcine	Value human	Comments
10	NO growth inhibition threshold	1000 nM [65,144]	Similar	In vitro cell cultures, murine and human mostly

Appendix B.
Vessel slices *in vivo* and *in silico*

In silico slices are rotated so that the outer curvature of the vessel is on top. Stent explanted (a) 14 days; (b) 28 days post-stenting. Slides order from proximal to distal. Letters denote strut IDs, see Figure 37. Blue areas show neointima estimation, as described in the paper. If the lumen is outside the area enclosed by the struts (see e.g. EF in the 1st *in vivo* slide), the area is taken as negative.

(a) 14 days (stent ID: JG929RCA)
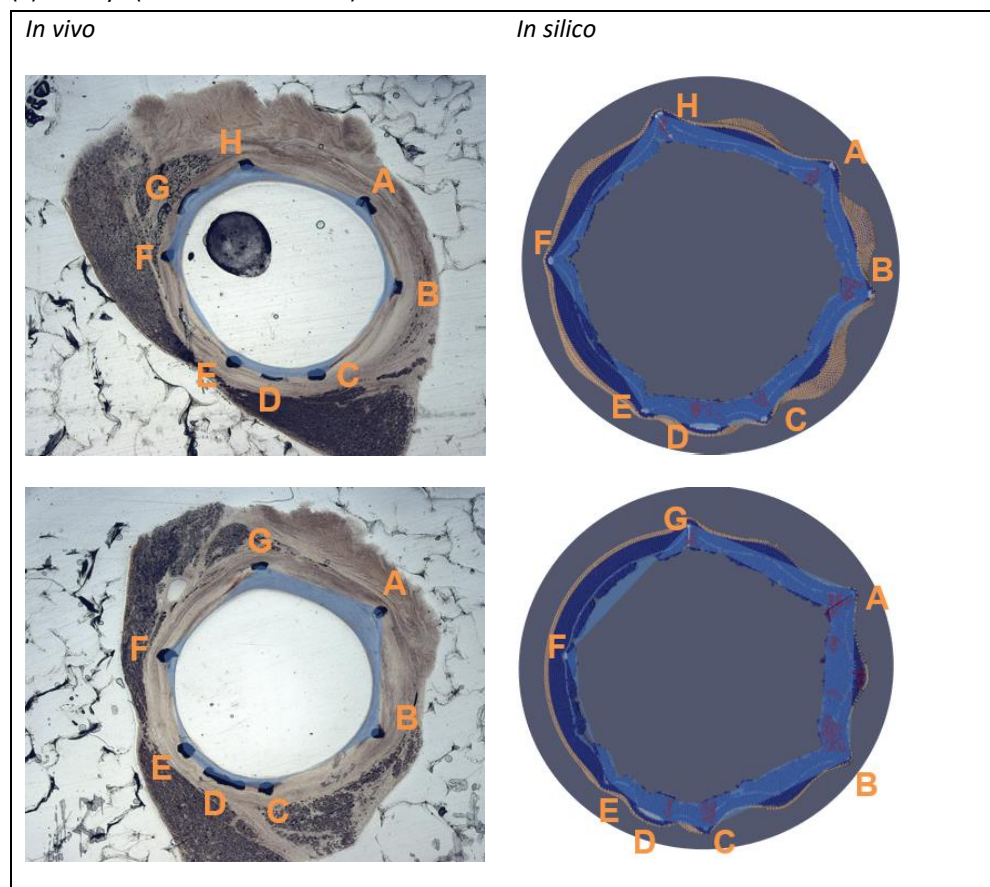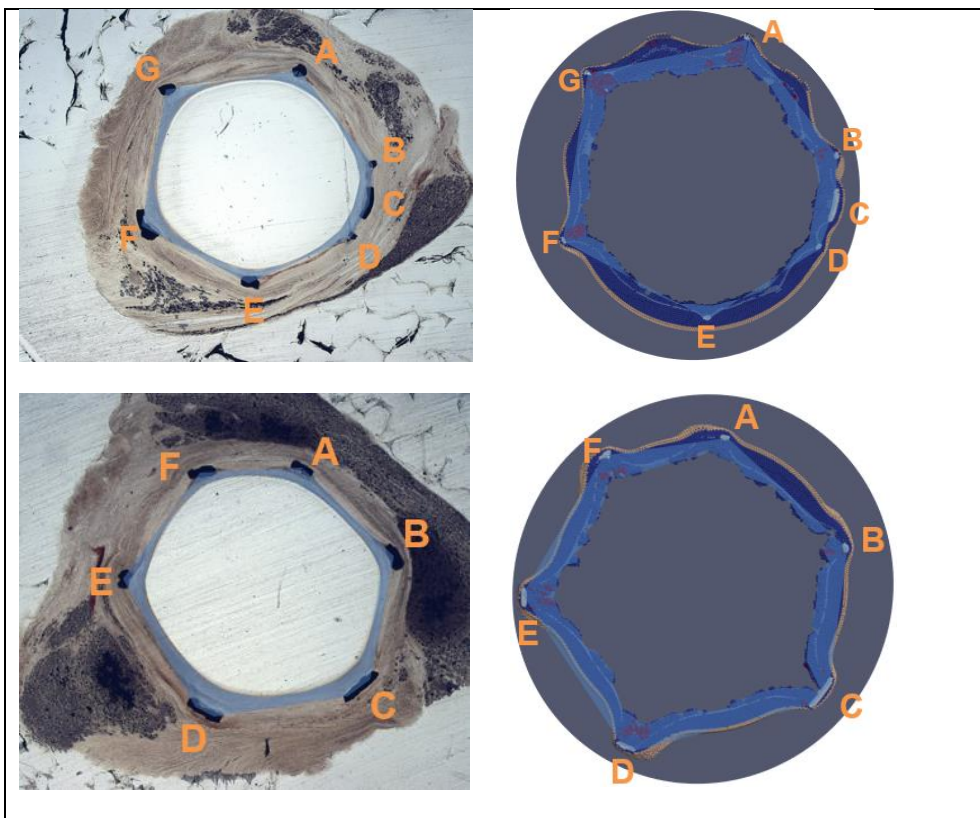
(b) 28 days (stent ID: JG931RCA)

In vivo   *In silico*
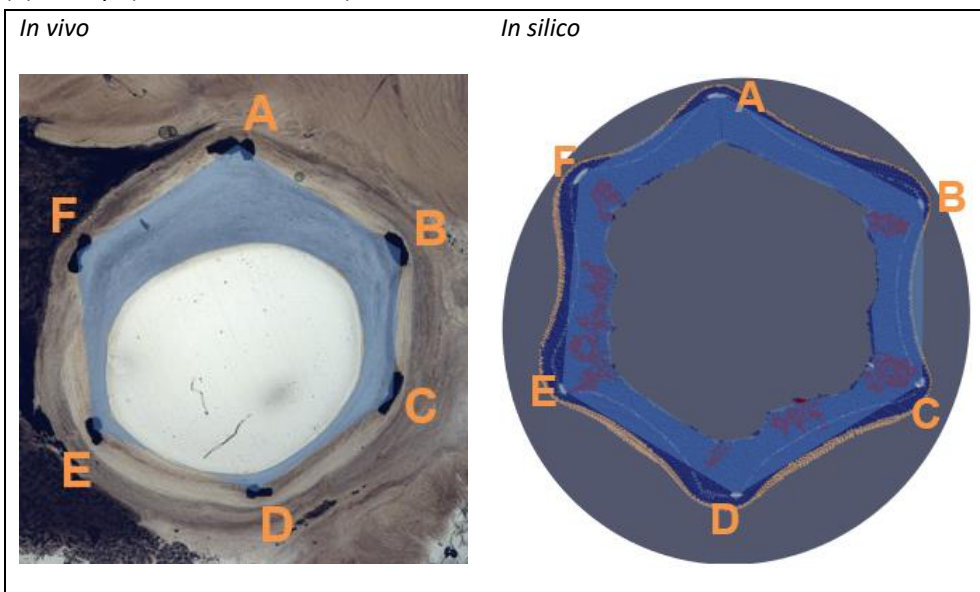
References

[1]   Tortora GJ, Funke BR, Case CL. Microbiology: an introduction. 2019.

[2]   Giovannoni SJ, Tripp HJ, Givan S, Podar M, Vergin KL, Baptista D, et al. Genome Streamlining in a Cosmopolitan Oceanic Bacterium. Science (80-) 2005;309:1242–5. doi:10.1126/science.1114057.

[3]   Sears R, Calambokidis J. Update COSEWIC status report on the Blue Whale Balaenoptera musculus in Canada, in COSEWIC assessment and update status report on the Blue Whale Balaenoptera musculus in Canada. Ottawa. Comm Status Endanger Wildl Canada Ottawa 2002:1–32.

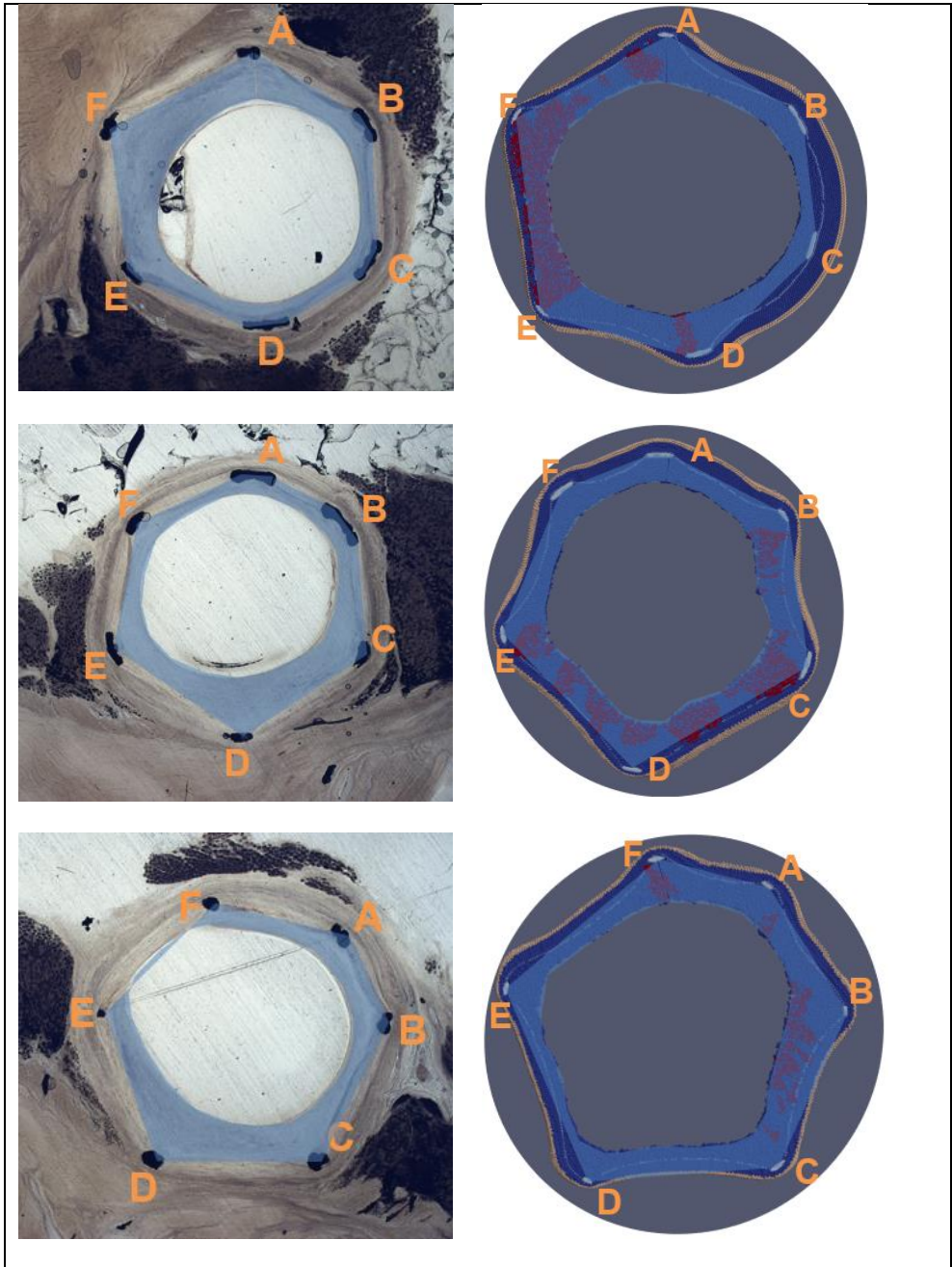[4]   Stephenson NL. Reference conditions for giant sequoia forest restoration: structure, process, and precision. vol. 9. 1999.

[5]   DeWoody J, Rowe CA, Hipkins VD, Mock KE. "Pando" Lives: Molecular Genetic Evidence of a Giant Aspen Clone in Central Utah. West North Am Nat 2009;68:493–7. doi:10.3398/1527-0904-68.4.493.

[6]   Hoekstra A, Chopard B, Coveney P. Multiscale modelling and simulation: A position paper. Philos Trans R Soc A Math Phys Eng Sci 2014;372:20130377. doi:10.1098/rsta.2013.0377.

[7]   Falcone JL, Chopard B, Hoekstra A. MML: Towards a multiscale modeling language. Procedia Comput Sci 2010;1:819–26. doi:10.1016/j.procs.2010.04.089.

[8]   Evans DJW, Lawford P V., Gunn J, Walker D, Hose DR, Smallwood RH, et al. The application of multiscale modelling to the process of development and prevention of stenosis in a stented coronary artery. Philos Trans R Soc A Math Phys Eng Sci 2008;366:3343–60. doi:10.1098/rsta.2008.0081.

[9]   Karabasov S, Nerukh D, Hoekstra A, Chopard B, Coveney P V. Multiscale modelling: Approaches and challenges. Philos Trans R Soc A Math Phys Eng Sci 2014;372:2–4. doi:10.1098/rsta.2013.0390.

[10]   Sutera SP, Skalak R. The History of Poiseuille's Law. Annu Rev Fluid Mech 1993;25:1–20.

[11]   Westerhof N, Lankhaar JW, Westerhof BE. The arterial windkessel. Med Biol Eng Comput 2009;47:131–41. doi:10.1007/s11517-008-0359-2.

[12]   Frank O. Die grundform des arteriellen pulses. Z Biol 1899;37:19.

[13]   Noble D. The future: putting Humpty-Dumpty together again. Biochem Soc Trans 2003;31:156–8. doi:10.1042/bst0310156.

[14]   Bassingthwaighte J. Toward modeling the human physionome. Adv Exp Med Biol 1995;382:331–9.

[15]   Ayache N, Boissel J, Brunak S, Clapworthy G, Fingberg J. Towards Virtual Physiological Human: multilevel modelling and simulation ofthe human anatomy and physiology. White Pap 2005;Eur. Comm.:1–29.

[16]   Viceconti M, Hunter P. The Virtual Physiological Human: Ten Years After. Annu Rev

Biomed Eng 2016;18:103–23. doi:10.1146/annurev-bioeng-110915-114742.

[17]   VPH Inst. From challenges to opportunities: towards a common strategic framework for EU Research and innovation funding. Position Pap n.d.:1–4.

[18]   Global Health Estimates 2016: Deaths by Cause, Age, Sex, by Country and by Region, 2000-2016. Geneva, World Health Organization: 2018.

[19]   Hoekstra AG, Alowayyed S, Lorenz E, Melnikova N, Mountrakis L, Rooij B van, et al. Towards the Virtual Artery: a Multiscale Model for Vascular Physiology at the PCB Interface. Phil Trans R Soc A 2016;374:20160146. doi:http://dx.doi.org/10.1098/rsta.2016.0146.

[20]   Boron WF, Boulpaep EL. Medical Physiology: A Cellular and Molecular Approach, updated second edition. Philadelphia: Saunders Elsevier; 2009.

[21]   Tarbell JM, Shi Z-D, Dunn J, Jo H. Fluid Mechanics, Arterial Disease, and Gene Expression. Annu Rev Fluid Mech 2014;46:591–614. doi:10.1146/annurev-fluid-010313-141309.

[22]   van de Vosse FN, Stergiopulos N. Pulse Wave Propagation in the Arterial Tree. Annu Rev Fluid Mech 2011;43:467–99. doi:10.1146/annurev-fluid-122109-160730.

[23]   Ostrowski MA, Huang NF, Walker TW, Verwijlen T, Poplawski C, Khoo AS, et al. Microvascular endothelial cells migrate upstream and align against the shear stress field created by impinging flow. Biophys J 2014;106:366–74. doi:10.1016/j.bpj.2013.11.4502.

[24]   Sriram K, Laughlin JG, Rangamani P, Tartakovsky DM. Shear-Induced Nitric Oxide Production by Endothelial Cells. Biophys J 2016;111:208–21. doi:10.1016/j.bpj.2016.05.034.

[25]   Tuttle JL, Nachreiner RD, Bhuller AS, Condict KW, Connors BA, Herring BP, et al. Shear level influences resistance artery remodeling : wall dimensions, cell density, and eNOS expression. Am J Physiol Heart Circ Physiol 2001;281:H1380–9.

[26]   Helisch A, Schaper W. Arteriogenesis: the development and growth of collateral arteries. Microcirculation 2003;10:83–97. doi:10.1038/sj.mn.7800173.

[27]   Zun PS, Hoekstra AG. On the Possible Interaction Mechanism between Collateral Vessels and Restenosis. Procedia Comput Sci 2015;66:412–8. doi:10.1016/j.procs.2015.11.047.

[28]   Svitenkov A, Pavlov I, Chivilikhin SA. A one-dimensional model of agent propagation in arterial blood flow. Procedia Comput Sci 2018;136:416–24. doi:10.1016/j.procs.2018.08.272.

[29]   Zun PS, Anikina T, Svitenkov A, Hoekstra AG. A Comparison of Fully-Coupled 3D In-Stent Restenosis Simulations to In-vivo Data. Front Physiol 2017;8:284. doi:10.3389/fphys.2017.00284.

[30]   Artoli AM, Hoekstra AG, Sloot PMA. Mesoscopic simulations of systolic flow in the human abdominal aorta. J Biomech 2006;39:873–84. doi:10.1016/j.jbiomech.2005.01.033.

[31]   Czaja B, Závodszky G, Azizi Tarksalooyeh V, Hoekstra AG. Cell-resolved blood flow simulations of saccular aneurysms: Effects of pulsatility and aspect ratio. J R Soc Interface 2018;15. doi:10.1098/rsif.2018.0485.

[32]   Niculescu I. Towards a cell-based model of Neointimal Hyperplasia with Cellular Potts Model. MSc thesis, UvA, 2011.

[33]   Melnikova NB, Svitenkov AI, Hose DR, Hoekstra AG. A cell-based mechanical model of coronary artery tunica media. J R Soc Interface 2017;14:20170028. doi:10.1098/rsif.2017.0028.

[34]   Tahir H, Bona-Casas C, Narracott AJ, Iqbal J, Gunn JP, Lawford P V., et al. Endothelial repair process and its relevance to longitudinal neointimal tissue patterns: comparing histology with in silico modelling. J R Soc Interface 2014;11:20140022. doi:http://dx.doi.org/10.1098/rsif.2014.0022.

[35]   Kovatchev B, Breton M, Dalla Man C, Cobelli C. In Silico Preclinical Trials: A Proof of Concept in Closed-Loop Control of Type 1 Diabetes. J Diabetes Sci Technol 2009;3:44–55.

[36]   Danad I, Baskaran L, Min JK. Noninvasive Fractional Flow Reserve Derived from Coronary Computed Tomography Angiography for the Diagnosis of Lesion-specific Ischemia. Interv Cardiol Clin 2015;4:481–9. doi:10.1016/j.iccl.2015.06.008.

[37]   Morris PD, van de Vosse FN, Lawford P V., Hose DR, Gunn JP. "Virtual" (Computed) Fractional Flow Reserve. JACC Cardiovasc Interv 2015;8. doi:10.1016/j.jcin.2015.04.006.

[38]   Morris PD, Ryan D, Morton AC, Lycett R, Lawford P V., Hose DR, et al. Virtual Fractional Flow Reserve From Coronary Angiography : Modeling the Significance of Coronary Lesions. JACC Cardiovasc Interv 2013;6:149–57. doi:10.1016/j.jcin.2012.08.024.

[39]   Iqbal J, Gunn JP, Serruys PW. Coronary stents: historical development, current status and future directions. Br Med Bull 2013;106:193–211. doi:10.1093/bmb/ldt009.

[40]   Jukema JW, Verschuren JJW, Ahmed TAN, Quax PHA. Restenosis after PCI. Part 1: pathophysiology and risk factors. Nat Rev Cardiol 2012;9:53–62. doi:10.1038/nrcardio.2011.132.

[41]   Jukema JW, Ahmed TAN, Verschuren JJW, Quax PHA. Restenosis after PCI. Part 2: prevention and therapy. Nat Rev Cardiol 2012;9:79–90. doi:10.1038/nrcardio.2011.148.

[42]   Chieffo A, Foglieni C, Nodari RL, Briguori C, Sangiorgi G, Latib A, et al. Histopathology of Clinical Coronary Restenosis in Drug-Eluting Versus Bare Metal Stents. Am J Cardiol 2009;104:1660–7. doi:10.1016/j.amjcard.2009.07.041.

[43]   Roache PJ. Verification and validation in computational science and engineering. Hermosa; 1998.

[44]   Tahir H, Bona-Casas C, Hoekstra AG. Modelling the effect of a functional endothelium on the development of in-stent restenosis. PLoS One 2013;8:e66138. doi:10.1371/journal.pone.0066138.

[45]   Lagerqvist B, Carlsson J, Fröbert O, Lindbäck J, Scherstén F, Stenestrand U, et al. Stent thrombosis in Sweden: a report from the Swedish Coronary Angiography and Angioplasty Registry. Circ Cardiovasc Interv 2009;2:401–8. doi:10.1161/CIRCINTERVENTIONS.108.844985.

[46]   Kolandaivelu K, Swaminathan R, Gibson WJ, Kolachalama VB, Nguyen-Ehrenreich K-L, Giddings VL, et al. Stent Thrombogenicity Early in High-Risk Interventional Settings Is Driven by Stent Design and Deployment and Protected by Polymer-Drug Coatings. Circulation 2011;123:1400–9.

doi:10.1161/CIRCULATIONAHA.110.003210.

[47] De Caterina AR, Cuculi F, Banning AP. Incidence, predictors and management of left main coronary artery stent restenosis: A comprehensive review in the era of drug-eluting stents. EuroIntervention 2013;8:1326–34. doi:10.4244/EIJV8I11A201.

[48] Giacoppo D, Gargiulo G, Aruta P, Capranzano P, Tamburino C, Capodanno D. Treatment strategies for coronary in-stent restenosis: systematic review and hierarchical Bayesian network meta-analysis of 24 randomised trials and 4880 patients. BMJ 2015;351:h5392. doi:10.1136/bmj.h5392.

[49] Goel SS, Gajulapalli RD, Athappan G, Gupta S, Ellis S, Tuzcu EM, et al. Management of drug eluting stent in-stent restenosis: A systematic review and meta-analysis. J Am Coll Cardiol 2013;62:B253. doi:10.1002/ccd.26151.

[50] Meier P, Indermuehle A, Pitt B, Traupe T, De Marchi SF, Crake T, et al. Coronary collaterals and risk for restenosis after percutaneous coronary interventions: a meta-analysis. BMC Med 2012;10:62. doi:10.1186/1741-7015-10-62.

[51] Nolan DR, Gower AL, Destrade M, Ogden RW, McGarry JP. A robust anisotropic hyperelastic formulation for the modelling of soft tissue. J Mech Behav Biomed Mater 2014;39:48–60. doi:10.1016/j.jmbbm.2014.06.016.

[52] Zahedmanesh H, Van Oosterwyck H, Lally C. A multi-scale mechanobiological model of in-stent restenosis: deciphering the role of matrix metalloproteinase and extracellular matrix changes. Comput Methods Biomech Biomed Engin 2014;17:813–28. doi:10.1080/10255842.2012.716830.

[53] Prendergast P, Lally C, Daly S, Reid AJ, Quinn D, Dolan F. Analysis of Prolapse in Cardiovascular Stents : A Constitutive Equation for Vascular Tissue and Finite-Element. Trans ASME 2003;125. doi:10.1115/1.1613674.

[54] Boyle CJ, Lennon AB, Prendergast PJ. Application of a mechanobiological simulation technique to stents used clinically. J Biomech 2013;46:918–24. doi:10.1016/j.jbiomech.2012.12.014.

[55] Boyle CJ, Lennon AB, Prendergast PJ. In Silico Prediction of the Mechanobiological Response of Arterial Tissue: Application to Angioplasty and Stenting. J Biomech Eng 2011;133:081001. doi:10.1115/1.4004492.

[56] Keller BK, Amatruda CM, Hose DR, Gunn JP, Lawford V, Dubini G, et al. Contribution of Mechanical and Fluid Stresses to the Magnitude of In-stent Restenosis at the Level of Individual Stent Struts. Cardiovasc Eng Technol 2014;5:164–75. doi:10.1007/s13239-014-0181-y.

[57] Tahir H, Hoekstra AG, Lorenz E, Lawford P V., Hose DR, Gunn JP, et al. Multi-scale simulations of the dynamics of in-stent restenosis: impact of stent deployment and design. Interface Focus 2011;1:365–73. doi:10.1098/rsfs.2010.0024.

[58] Amatruda CM, Bona-Casas C, Keller BK, Tahir H, Dubini G, Hoekstra AG, et al. From histology and imaging data to models for in-stent restenosis. Int J Artif Organs 2014;37:786–800. doi:10.5301/ijao.5000336.

[59] Tahir H, Niculescu I, Bona-Casas C, Merks RMH, Hoekstra AG. An in silico study on the role of smooth muscle cell migration in neointimal formation after coronary stenting. J R Soc Interface 2015;12:20150358. doi:10.1098/rsif.2015.0358.

[60] Morton AC, Arnold ND, Crossman DC, Gunn JP. Response of very small (2 mm) porcine coronary arteries to balloon angioplasty and stent implantation. Heart

2004;90:324–7. doi:10.1136/hrt.2003.015305.

[61]   Gunn JP, Arnold ND, Chan KH, Shepherd L, Cumberland DC, Crossman DC. Coronary artery stretch versus deep injury in the development of in-stent neointima. Hear 2002;88:401–5. doi:10.1136/heart.88.4.401.

[62]   Caiazzo A, Evans D, Falcone JL, Hegewald J, Lorenz E, Stahl B, et al. A Complex Automata approach for in-stent restenosis: Two-dimensional multiscale modelling and simulations. J Comput Sci 2011;2:9–17. doi:10.1016/j.jocs.2010.09.002.

[63]   Chopard B, Borgdorff J, Hoekstra AG. A framework for multi-scale modelling. Philos Trans R Soc A Math Phys Eng Sci 2014;372:20130378. doi:http://dx.doi.org/10.1098/rsta.2013.0378.

[64]   Groen D, Borgdorff J, Bona-Casas C, Hetherington J, Nash RW, Zasada SJ, et al. Flexible composition and execution of high performance, high fidelity multiscale biomedical simulations. Interface Focus 2013;3:20120087. doi:10.1098/rsfs.2012.0087.

[65]   Coneski PN, Schoenfisch MH. Nitric oxide release: Part III. Measurement and reporting. Chem Soc Rev 2012;41:3753. doi:10.1039/c2cs15271a.

[66]   Holzapfel GA, Sommer G, Gasser CT, Regitnig P. Determination of layer-specific mechanical properties of human coronary arteries with nonatherosclerotic intimal thickening and related constitutive modeling. Am J Physiol - Hear Circ Physiol 2005;289:2048–58. doi:10.1152/ajpheart.00934.2004.

[67]   Kwon HM, Sangiorgi G, Spagnoli L, Miyauchi K, Holmes DR, Schwartz RS, et al. Experimental hypercholesterolemia induces ultrastructural changes in the internal elastic lamina of porcine coronary arteries. Atherosclerosis 1998;139:283–9.

[68]   Palabos 2013.

[69]   Ku DN. Blood Flow in Arteries. Annu Rev Fluid Mech 1997;29:399–434. doi:10.1146/annurev.fluid.29.1.399.

[70]   Axner L, Hoekstra AG, Jeays A, Lawford P, Hose R, Sloot PM a. Simulations of time harmonic blood flow in the Mesenteric artery: comparing finite element and lattice Boltzmann methods. Biomed Eng Online 2009;8:23. doi:10.1186/1475-925X-8-23.

[71]   Iqbal J, Chamberlain J, Francis SE, Gunn J. Role of Animal Models in Coronary Stenting. Ann Biomed Eng 2016;44:453–65. doi:10.1007/s10439-015-1414-4.

[72]   Nakazawa G, Granada JF, Alviar CL, Tellez A, Kaluza GL, Guilhermier MY, et al. Anti-CD34 Antibodies Immobilized on the Surface of Sirolimus-Eluting Stents Enhance Stent Endothelialization. JACC Cardiovasc Interv 2010;3:68–75. doi:10.1016/j.jcin.2009.09.015.

[73]   Van Beusekom HMM, Ertaş G, Sorop O, Serruys PW, Van Der Giessen WJ. The Genous™ endothelial progenitor cell capture stent accelerates stent re-endothelialization but does not affect intimal hyperplasia in porcine coronary arteries. Catheter Cardiovasc Interv 2012;79:231–42. doi:10.1002/ccd.22928.

[74]   Schwartz RS, Chu A, Edwards WD, Srivatsa SS, Simari RD, Isner JM, et al. A proliferation analysis of arterial neointimal hyperplasia: Lessons for antiproliferative restenosis therapies. Int J Cardiol 1996;53:71–80. doi:10.1016/0167-5273(95)02499-9.

[75]   Briguori C, Sarais C, Pagnotta P, Liistro F, Montorfano M, Chieffo A, et al. In-stent restenosis in small coronary arteries. J Am Coll Cardiol 2002;40:403–9.

doi:10.1016/S0735-1097(02)01989-7.

[76]   Borgdorff J, Ben Belgacem M, Bona-Casas C, Fazendeiro L, Groen D, Hoenen O, et al. Performance of distributed multiscale simulations. Philos Trans R Soc A Math Phys Eng Sci 2014;372:20130407. doi:10.1098/rsta.2013.0407.

[77]   Duraiswamy N, Schoephoerster RT, Moreno MR, Moore JE. Stented Artery Flow Patterns and Their Effects on the Artery Wall. Annu Rev Fluid Mech 2007;39:357–82. doi:10.1146/annurev.fluid.39.050905.110300.

[78]   Farb A, Kolodgie FD, Hwang JY, Burke AP, Tefera K, Weber DK, et al. Extracellular matrix changes in stented human coronary arteries. Circulation 2004;110:940–7. doi:10.1161/01.CIR.0000139337.56084.30.

[79]   Parton A, McGilligan V, O'Kane M, Baldrick FR, Watterson S. Computational modelling of atherosclerosis. Brief Bioinform 2016;17:562–75. doi:10.1093/bib/bbv081.

[80]   DeMaio L, Tarbell JM, Scaduto RC, Gardner TW, Antonetti D a. A transmural pressure gradient induces mechanical and biological adaptive responses in endothelial cells. Am J Physiol Heart Circ Physiol 2004;286:H731-41. doi:10.1152/ajpheart.00427.2003.

[81]   Witthoft A, Yazdani A, Peng Z, Bellini C, Humphrey JD, Karniadakis GE. A discrete mesoscopic particle model of the mechanics of a multi-constituent arterial wall. J R Soc Interface 2016;13:20150964-. doi:10.1098/rsif.2015.0964.

[82]   Kim WH, Hong MK, Virmani R, Kornowski R, Jones R, Leon MB. Histopathologic analysis of in-stent neointimal regression in a porcine coronary model. Coron Artery Dis 2000;11:273–7. doi:10.1097/00019501-200005000-00011.

[83]   Iqbal J, Serruys PW, Taggart DP. Optimal revascularization for complex coronary artery disease. Nat Rev Cardiol 2013;10:635–47. doi:10.1038/nrcardio.2013.138.

[84]   Fernández-Ruiz I. Interventional cardiology: Drug-eluting or bare-metal stents? Nat Rev Cardiol 2016;13:631–631. doi:10.1038/nrcardio.2016.160.

[85]   Ghasemi M, Nolan DR, Lally C. An investigation into the role of different constituents in damage accumulation in arterial tissue and constitutive model development. Biomech Model Mechanobiol 2018;17:1757–69. doi:10.1007/s10237-018-1054-3.

[86]   Keshavarzian M, Meyer CA, Hayenga HN. Mechanobiological model of arterial growth and remodeling. Biomech Model Mechanobiol 2017;17:1–15. doi:10.1007/s10237-017-0946-y.

[87]   Smith RC. Uncertainty quantification: theory, implementation, and applications. SIAM; 2013.

[88]   Nikishova A, Veen L, Zun P, Hoekstra AG. Uncertainty Quantification of a Multiscale Model for In-Stent Restenosis. Cardiovasc Eng Technol 2018;9:761–74. doi:10.1007/s13239-018-00372-4.

[89]   Mathelin L, Hussaini MY, Zang TA. Stochastic approaches to uncertainty quantification in CFD simulations. Numer Algorithms 2005;38:209–36. doi:10.1007/s11075-004-2866-z.

[90]   Alowayyed S, Groen D, Coveney P V., Hoekstra AG. Multiscale computing in the exascale era. J Comput Sci 2017;22:15–25. doi:10.1016/j.jocs.2017.07.004.

[91]   Nikishova A, Veen L, Zun P, Hoekstra AG. Semi-intrusive multiscale metamodelling uncertainty quantification with application to a model of in-stent restenosis. Philos

Trans R Soc A Math Phys Eng Sci 2019;377:20180154. doi:10.1098/rsta.2018.0154.

[92]   Serruys PW, Ormiston JA, Onuma Y, Regar E, Gonzalo N, Garcia-Garcia HM, et al. A bioabsorbable everolimus-eluting coronary stent system (ABSORB): 2-year outcomes and results from multiple imaging methods. Lancet 2009;373:897–910. doi:10.1016/S0140-6736(09)60325-1.

[93]   Ofili EO, Kern MJ, Labovitz AJ, St Vrain JA, Segal J, Aguirre F V, et al. Analysis of coronary blood flow velocity dynamics in angiographically normal and stenosed arteries before and after endolumen enlargement by angioplasty. J Am Coll Cardiol 1993;21:308–16. doi:10.1016/0735-1097(93)90668-Q.

[94]   Sobol IM. On sensitivity estimation for nonlinear mathematical models. Mat Model 1990;2:112–8. doi:10.18287/0134-2452-2015-39-4-459-461.

[95]   Sobol IM. On quasi-Monte Carlo integrations. Math Comput Simul 1998;47:103–12. doi:10.1016/s0378-4754(98)00096-2.

[96]   Douglas G, Van Kampen E, Hale AB, McNeill E, Patel J, Crabtree MJ, et al. Endothelial cell repopulation after stenting determines in-stent neointima formation: Effects of bare-metal vs. drug-eluting stents and genetic endothelial cell modification. Eur Heart J 2013;34:3378–88. doi:10.1093/eurheartj/ehs240.

[97]   Chaabane C, Otsuka F, Virmani R, Bochaton-Piallat ML. Biological responses in stented arteries. Cardiovasc Res 2013;99:353–63. doi:10.1093/cvr/cvt115.

[98]   Tardy Y, Resnick N, Nagel T, Gimbrone MA, Dewey CF. Shear Stress Gradients Remodel Endothelial Monolayers in Vitro via a Cell Proliferation-Migration-Loss Cycle. Arterioscler Thromb Vasc Biol 1997;17:3102–6. doi:https://doi.org/10.1161/01.ATV.17.11.3102.

[99]   Hsiao ST, Spencer T, Boldock L, Prosseda SD, Xanthis I, Tovar-Lopez FJ, et al. Endothelial repair in stented arteries is accelerated by inhibition of Rho-associated protein kinase. Cardiovasc Res 2016;112:1–13. doi:10.1093/cvr/cvw210.

[100] DePaola N, Gimbrone MA, Davies PF, Dewey CF. Vascular endothelium responds to fluid shear stress gradients. Arterioscler Thromb Vasc Biol 1992;12:1254–7. doi:10.1161/01.ATV.12.11.1254.

[101] Teichmann J, Morgenstern A, Seebach J, Schnittler HJ, Werner C, Pompe T. The control of endothelial cell adhesion and migration by shear stress and matrix-substrate anchorage. Biomaterials 2012;33:1959–69. doi:10.1016/j.biomaterials.2011.11.017.

[102] Lee Y, Kouvroukoglou S, McIntire L V., Zygourakis K. A cellular automaton model for the proliferation of migrating contact-inhibited cells. Biophys J 1995;69:1284–98. doi:10.1016/S0006-3495(95)79996-9.

[103] Kruger T. The lattice boltzmann method. 2017. doi:10.1007/978-3-319-44649-3.

[104] Malek AM, Alper SL, Izumo S. Hemodynamic Shear Stress and Its Role in Atherosclerosis. JAMA 1999;282:2035–42.

[105] Dabagh M, Jalali P, Butler PJ, Randles A, Tarbell JM. Mechanotransmission in endothelial cells subjected to oscillatory and multi-directional shear flow. J R Soc Interface 2017;14. doi:10.1098/rsif.2017.0185.

[106] Timraz SBH, Farhat IAH, Alhussein G, Christoforou N, Teo JCM. In-depth evaluation of commercially available human vascular smooth muscle cells phenotype: Implications for vascular tissue engineering. Exp Cell Res 2016;343:168–76.

doi:10.1016/j.yexcr.2016.04.004.

[107] Stegemann JP, Nerem RM. Altered response of vascular smooth muscle cells to exogenous biochemical stimulation in two- and three-dimensional culture. Exp Cell Res 2003;283:146–55. doi:10.1016/S0014-4827(02)00041-1.

[108] Morlacchi S, Keller BK, Arcangeli P, Balzan M, Migliavacca F, Dubini G, et al. Hemodynamics and In-stent restenosis: Micro-CT images, histology, and computer simulations. Ann Biomed Eng 2011;39:2615–26. doi:10.1007/s10439-011-0355-9.

[109] Nolan DR, Lally C. An investigation of damage mechanisms in mechanobiological models of in-stent restenosis. J Comput Sci 2018;24:132–42. doi:10.1016/j.jocs.2017.04.009.

[110] Werner GS, Fritzenwanger M, Prochnau D, Schwarz G, Ferrari M, Aarnoudse W, et al. Determinants of Coronary Steal in Chronic Total Coronary Occlusions. Donor Artery, Collateral, and Microvascular Resistance. J Am Coll Cardiol 2006;48:51–8. doi:10.1016/j.jacc.2005.11.093.

[111] Taylor CA, Fonte TA, Min JK. Computational fluid dynamics applied to cardiac computed tomography for noninvasive quantification of fractional flow reserve: Scientific basis. J Am Coll Cardiol 2013;61:2233–41. doi:10.1016/j.jacc.2012.11.083.

[112] Caputo M, Chiastra C, Cianciolo C, Cutrì E, Dubini G, Gunn J, et al. Simulation of oxygen transfer in stented arteries and correlation with in-stent restenosis. Int j Numer Method Biomed Eng 2013;29:1373–87. doi:10.1002/cnm.2588.

[113] Chatzizisis YS, Coskun AU, Jonas M, Edelman ER, Stone PH, Feldman CL. Risk stratification of individual coronary lesions using local endothelial shear stress: a new paradigm for managing coronary artery disease. Curr Opin Cardiol 2007;22:552–64. doi:10.1097/HCO.0b013e3282f07548.

[114] Boileau E, Nithiarasu P. One-Dimensional Modelling of the Coronary Circulation. Application to Noninvasive Quantification of Fractional Flow Reserve (FFR). Tavares J., Natal Jorge R. Comput. Exp. Biomed. Sci. Methods Appl. Lect. Notes Comput. Vis. Biomech. vol 21, 2015, p. 137–55. doi:10.1007/978-3-319-15799-3_11.

[115] Gamilov TM, Kopylov PY, Pryamonosov RA, Simakov SS. Virtual fractional flow reserve assessment in patient-specific coronary networks by 1D hemodynamic model. Russ J Numer Anal Math Model 2015;30:269–76. doi:10.1515/rnam-2015-0024.

[116] Grewe PH, Deneke T, Machraoui A, Barmeyer J, Müller K-M. Acute and Chronic Tissue Response to Coronary Stent Implantation: Pathologic Findings in Human Specimen. 2000. doi:10.1016/S0735-1097(99)00486-6.

[117] Malik N, Gunn JP, Holt CM, Shepherd L, Francis SE, Newman CMH, et al. Intravascular stents: a new technique for tissue processing for histology, immunohistochemistry, and transmission electron microscopy. Heart 1998;80:509–16. doi:10.1136/hrt.80.5.509.

[118] Murphy SL, Xu J, Kochanek KD, Curtin SC, Arias E. Deaths: Final data for 2015. Natl Vital Stat Reports 2017;66. doi:10.1136/vr.h753.

[119] Stefanini GG, Byrne RA, Windecker S, Kastrati A. State of the art: Coronary artery stents - Past, present and future. EuroIntervention 2017;13:706–16. doi:10.4244/EIJ-D-17-00557.

[120] LaDisa JF, Olson LE, Molthen RC, Hettrick DA, Pratt PF, Hardel MD, et al. Alterations

in wall shear stress predict sites of neointimal hyperplasia after stent implantation in rabbit iliac arteries. Am J Physiol Circ Physiol 2005;288:H2465–75. doi:10.1152/ajpheart.01107.2004.

[121]   Bennett MR, Angelin S, McEwan JP, Jagoe R, Newby A. Inhibition of vascular smooth muscle cell proliferation in vitro and in vivo by c-myc antisense oligoeoxynucleotides. J Clin Invest 1994;93:820–8.

[122]   Zahedmanesh H, Lally C. A multiscale mechanobiological modelling framework using agent-based models and finite element analysis: Application to vascular tissue engineering. Biomech Model Mechanobiol 2012;11:363–77. doi:10.1007/s10237-011-0316-0.

[123]   Kenagy RD, Fischer JW, Lara S, Sandy JD, Clowes AW, Wight TN. Accumulation and Loss of Extracellular Matrix During Shear Stress-mediated Intimal Growth and Regression in Baboon Vascular Grafts. J Histochem Cytochem 2005;53:131–40. doi:10.1369/jhc.4A6493.2005.

[124]   Garratt KN, Edwards WD, Kaufmann UP, Vlietstra RE, Holmes DR. Differential histopathology of primary atherosclerotic and restenotic lesions in coronary arteries and saphenous vein bypass grafts: analysis of tissue obtained from 73 patients by directional atherectomy. J Am Coll Cardiol 1991;17:442–8. doi:10.1016/S0735-1097(10)80113-5.

[125]   Wight T, Lara S, Riessen R, Le Baron R, Isner J. Selective deposits of versican in the extracellular matrix of restenotic lesions from human peripheral arteries. Am J Pathol 1997;151:963–73.

[126]   Wight TN, Merrilees MJ. Proteoglycans in atherosclerosis and restenosis: Key roles for versican. Circ Res 2004;94:1158–67. doi:10.1161/01.RES.0000126921.29919.51.

[127]   Lee RT, Yamamoto C, Feng Y, Potter-Perigo S, Briggs WH, Landschulz KT, et al. Mechanical Strain Induces Specific Changes in the Synthesis and Organization of Proteoglycans by Vascular Smooth Muscle Cells. J Biol Chem 2001;276:13847–51. doi:10.1074/jbc.M010556200.

[128]   Curcio A, Torella D, Indolfi C. Mechanisms of Smooth Muscle Cell Proliferation and Endothelial Regeneration After Vascular Injury and Stenting. Circ J 2011;75:1287–96. doi:10.1253/circj.CJ-11-0366.

[129]   Succi S. The lattice Boltzmann equation for Fluid Dynamics and Beyond. Oxford Univ Press 2001:299. doi:10.1016/0370-1573(92)90090-M.

[130]   Messenger JC, Chen SYJ, Carroll JD, Burchenal JEB, Kioussopoulos K, Groves BM. 3D coronary reconstruction from routine single-plane coronary angiograms: Clinical validation and quantitative analysis of the right coronary artery in 100 patients. Int J Card Imaging 2000;16:413–27. doi:10.1023/A:1010643426720.

[131]   Keller BK. In-stent restenosis and coronary curvature: Translational approach to computational fluid dynamics. 2012.

[132]   Colombo A, Guha S, Mackle JN, Cahill PA, Lally C. Cyclic strain amplitude dictates the growth response of vascular smooth muscle cells in vitro: Role in in-stent restenosis and inhibition with a sirolimus drug-eluting stent. Biomech Model Mechanobiol 2013;12:671–83. doi:10.1007/s10237-012-0433-4.

[133]   Antoniadis AP, Mortier P, Kassab G, Dubini G, Foin N, Murasato Y, et al. Biomechanical Modeling to Improve Coronary Artery Bifurcation Stenting: Expert

Review Document on Techniques and Clinical Implementation. JACC Cardiovasc Interv 2015;8:1281–96. doi:10.1016/j.jcin.2015.06.015.

[134] Chiastra C, Migliori S, Burzotta F, Dubini G, Migliavacca F. Patient-Specific Modeling of Stented Coronary Arteries Reconstructed from Optical Coherence Tomography: Towards a Widespread Clinical Use of Fluid Dynamics Analyses. J Cardiovasc Transl Res 2018;11:156–72. doi:10.1007/s12265-017-9777-6.

[135] InSilc project n.d. https://insilc.eu/.

[136] Reymond P, Merenda F, Perren F, Ru D. Validation of a One-Dimensional Model of the Systemic Arterial Tree. Am J Physiol - Hear Circ Physiol 2009;297:208–22. doi:10.1152/ajpheart.00037.2009.

[137] Dodge JT, Brown BG, Bolson EL, Dodge HT. Lumen diameter of normal human coronary arteries. Influence of age, sex, anatomic variation, and left ventricular hypertrophy or dilation. Circulation 1992;86:232–46. doi:10.1161/01.CIR.86.1.232.

[138] Tahir H. Modelling and Simulating the Dynamics of In-Stent Restenosis in Porcine Coronary Arteries. PhD thesis, UvA, 2013.

[139] Huo Y, Choy JS, Svendsen M, Sinha AK, Kassab GS. Effects of vessel compliance on flow pattern in porcine epicardial right coronary arterial tree. J Biomech 2009;42:594–602. doi:10.1016/j.jbiomech.2008.12.011.

[140] Tantini B, Manes A, Fiumana E, Pignatti C, Guarnieri C, Zannoli R, et al. Antiproliferative effect of sildenafil on human pulmonary artery smooth muscle cells. Basic Res Cardiol 2005;100:131–8. doi:10.1007/s00395-004-0504-5.

[141] Tanner FC, Meier P, Greutert H, Champion C, Nabel EG, Lüscher TF. Nitric Oxide Modulates Expression of Cell Cycle Regulatory Proteins. Circulation 2000;101:1982–9. doi:10.1161/01.cir.101.16.1982.

[142] Grainger D, Kirschenlohr H, Metcalfe J, Weissberg P, Wade D, Lawn R. Proliferation of human smooth muscle cells promoted by lipoprotein(a). Science (80-) 1993;260:1655–8. doi:10.1126/science.8503012.

[143] Guo X, Kassab GS. Role of shear stress on nitrite and NOS protein content in different size conduit arteries of swine. Acta Physiol 2009;197:99–106. doi:10.1111/j.1748-1716.2009.01999.x.

[144] Thomas DD, Ridnour LA, Isenberg JS, Flores-Santana W, Switzer CH, Donzellie S, et al. The chemical biology of nitric oxide. Implications in celular signaling. Free Radic Biol Med 2008;45:18–31. doi:10.1016/j.freeradbiomed.2008.03.020.The.